Absolute neutron and photon flux characterization in the CNESTEN's TRIGA Mark II research reactor

H. Ghninou[1,*], A. Gruel[1], A. Lyoussi[1], C. Reynard-Carette[2], C. El Younoussi[3], B. El Bakkari[3], Y. Boulaich[3]

[1]CEA, DES, IRESNE, DER (SPESI/LP2E), Cadarache F-13108 Saint-Paul-Lez-Durance, France
[2]Aix Marseille Univ, Université de Toulon, CNRS, IM2NP, Marseille, France
[3] CNESTEN/CENM, POB 1382, Rabat, Morocco
(*) hamza.ghninou@cea.fr

***Abstract*— The National Center for Nuclear Energy, Sciences and Technology (CNESTEN) located in Rabat, Morocco, operates a 2 MW TRIGA Mark II research reactor. This type of reactor is specially designed to effectively implement the various fields of nuclear research such as neutron activation analysis, neutron radiography, detectors testing, radioisotopes production as well as education and training. In the last few years, a collaboration between the French Atomic Energy and Alternative Energies Commission (CEA) and the CNESTEN was established to expand the utilization of the TRIGA computational model by carrying out new in-situ measurements in order to characterize neutron and photon fields within and beyond the TRIGA reactor core. These new measurements will consolidate the knowledge of neutron and photon fluxes in different irradiation and instrumentation channels. The results of these experiments will also be used to extend the experimental validation of the new developed TRIPOLI-4® computational model of the reactor and to quantify the uncertainties and biases. This paper focuses on the neutron and photon flux characterization of two irradiation channels inside the TRIGA reactor core. Neutron measurements are ensured by activation dosimetry whereas photon measurements are ensured by thermo-luminescent detectors (TLD400 – CaF_2: Mn). Based on these techniques, the experiments were carried out during an experimental campaign conducted in June 2022. Preceding the implementation of these measurements, two experimental devices were specifically designed and manufactured to ensure a reproducible positioning of the detectors in the selected irradiation channels. This paper presents the experimental results analysis and the associated uncertainty quantification. These results will be then compared to the calculation ones obtained by the computational models of the TRIGA reactor.**

***Keywords* —In-core measurements, TRIGA reactor, Activation detectors, TLD detectors, Ionization chamber.**

I. Introduction

The TRIGA Mark II research reactor at the National Center for Energy, Sciences and Technology (CNESTEN) is a typical 2 MW TRIGA reactor which achieved its initial criticality on 02 May, 2007. It is a light water pool-type research reactor cooled by natural convection. Schematic drawings of the reactor core configuration are displayed in Fig. 1 and Fig. 2. The reactor core is immerged into an 8 m high and 2.52 m diameter tank filled with water and surrounded by a 21 cm thick cylindrical graphite block. The reactor core assembly consists of 101 FEs (including 5 fuel-follower control rods), 17 graphite elements, a central thimble (CT), a pneumatic transfer system (PTS) and a new irradiation channel located in the G25 location (cf. Fig. 2). The reactor is also equipped with a rotary specimen rack (RSR) containing 40 irradiation positions, a thermal column and four beam channels penetrating the concrete shield, the aluminum tank, and the reactor tank. Beam port NB1 is a tangential port, whereas beam ports NB2 – 4 are radially oriented. The TRIGA reactor fuel consists of a uniform mixture of uranium (8.5 %wt, enriched to 19.7% of ^{235}U) and zirconium hydride and it is contained in stainless steel cylindrical elements of approximately 73.2 cm in length and 3.6 cm in diameter. Similar to many other research reactors, the CNESTEN's TRIGA is designed to effectively implement a wide range of applications, including the production of radioisotopes for medical and industrial purposes [1] [2], qualification, under irradiation, fuel materials, inert materials and sensors [3] [4] [5] [6], validation and qualification of modelling and simulation tools [7] [8] [9] [10] [11] [12]. The implementation of such applications requires a reliable characterization of the neutron and photon fluxes in the reactor core. Indeed, the knowledge of neutron and photon fluxes is crucial for planning and carrying out experimental programs and for validating and qualifying computational models of the reactor. In fact, the first validation of the CNESTEN's TRIGA computational model was done by comparing the MCNP [13] calculated multiplication factor and control rod reactivity worth with the criticality benchmark experiments carried out in 2007 [14]. Up until then, this had been the only available validation of the computational model of the TRIGA reactor. Therefore, a new set of measurements was carried out in the TRIGA reactor core as part of the bilateral collaboration between CEA Cadarache, CNESTEN, and the joint laboratory LIMMEX (Aix-Marseille University, CEA, and CNRS). The primary objective of this collaboration is to expand the experimental validation of the TRIGA reactor by performing, analyzing, and interpreting experiments for the characterization of the irradiation and instrumentation channels. These measurements consist of three types of detectors: activation detectors for neutron characterization, thermo-luminescent detectors and a miniature ionization chamber for photon characterization. This decision was based on several criteria, including feedback from the use of these detectors in nuclear research reactors, such as detector dimensions, measurement uncertainties, and analysis and interpretation methods. It also considered the unique features of the TRIGA reactor and the associated irradiation constraints, such as the

dimensions of the irradiation channels and the levels of neutron and photon flux.

The present paper describes the neutron and photon flux characterization of two in-core irradiation channels of the CNESTEN's TRIGA Mark II research reactor. For each type of measurement, the obtained results are analyzed and the associated uncertainties are evaluated.

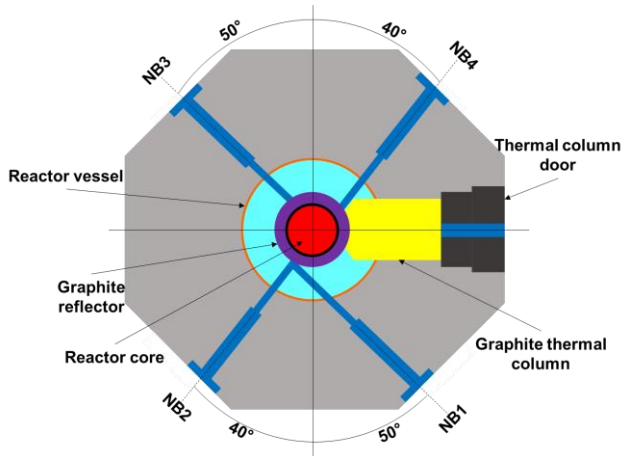

Fig. 1. Radial view of the CNESTEN's TRIGA reactor.

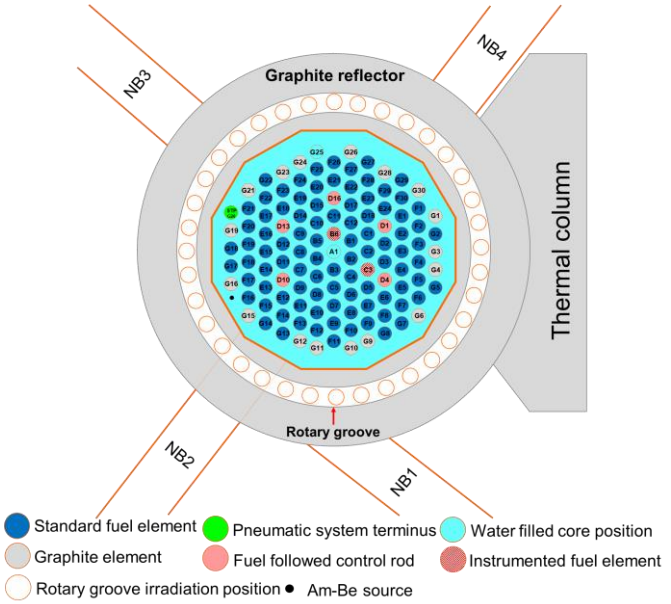

Fig. 2. Radial view of the TRIGA reactor core in the current operating configuration.

II. Measurements Design

A. Experimental set-up

As mentioned above, the TRIGA reactor is equipped with different irradiation channels that have different characteristics in terms of neutron flux levels and energy spectra. For this study, our aim is to characterize two in-core irradiation channels:

- CT: a water-filled irradiation channel located in the core center. It is an aluminum tube with, respectively, 3.2 and 3.4 internal and external diameters and 8 m length.
- G25: a new water-filled irradiation channel located at the core periphery, which has approximately the same diameter as the CT.

Three types of detectors were used to characterize the neutron and photon in different axial position in the irradiation channels: activation detectors, thermos-luminescent detectors and ionization chamber (cf. B). Carrying out of such measurements requires dedicated experimental devices to ensure the reproducibility of the measurements in the reactor. Schematic drawings of the experimental devices used in this study are presented in Fig. 3 and Fig. 4.

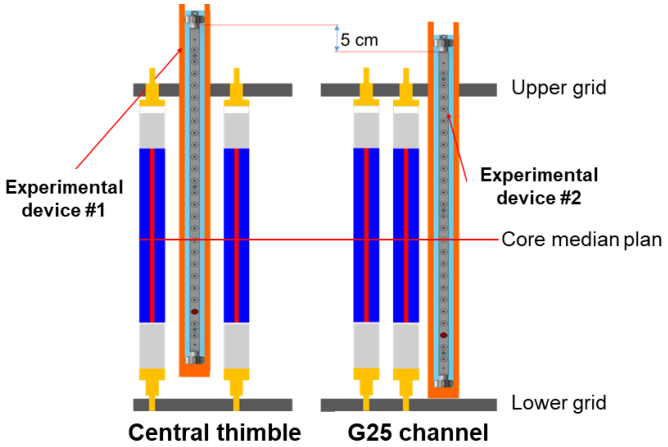

Fig. 3. Schematic of the experimental devices that were used to position activation and TLD dosimeters in the CT and G25 irradiation channels.

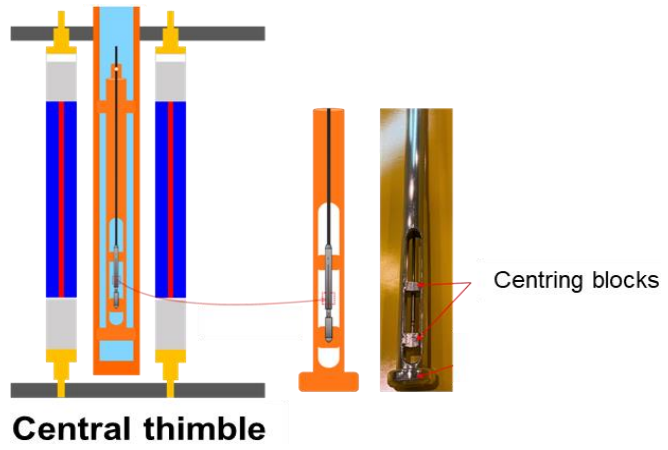

Fig. 4. Schematic of the positioning system used to place the MIC in the CT and G25 irradiation channels.

B. Experimental design

In the following paragraphs, the characteristics of the different detectors used in this study are described.

1) Activation detectors

For neutron flux measurements, we used two types of activation detectors to cover different energy regions of the neutron spectra: ^{59}Co(n, γ) and ^{58}Ni(n,p). The selection of these dosimeters is based on different criteria such as the cross section of the neutron reaction of interest, energy range of response, energy and intensity of decay γ rays' emission. The experimental design and the preliminary calculations are presented in [15]. At the end of irradiation, the analysis of the irradiated dosimeters is performed by means of the γ spectrometry technique using the CNESTEN's HP-Ge detector (cf. Fig. 5).

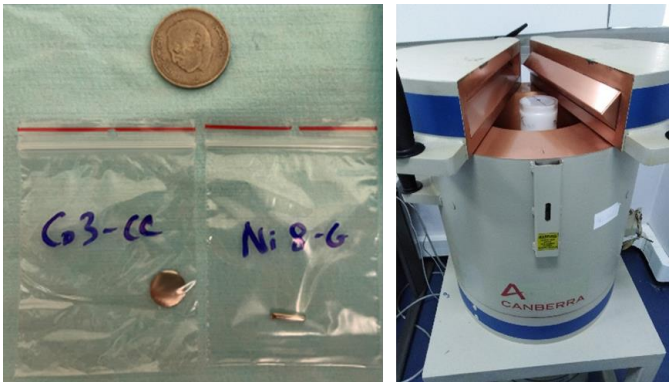

Fig. 5. (Left) cobalt and nickel dosimeters, (right) HPGe detector used for spectrometry γ measurements.

Two irradiations at two steady state power levels, 10 kW and 20 kW, were carried out. Table I presents the characteristics of the irradiations performed in the CT and G25 irradiation channel.

TABLE I
IRRADIATIONS CARRIED OUT IN CT AND G25 CHANNELS.

Date of irradiation	IC[2]	Power level	Irradiation time	Irradiated samples
09/12/2020	CT	20 kW	15 min	9 Ni
10/06/2022	CT G25	10 kW	15 min	19 Co 10 Co and 9 Ni

[2] IC : Irradiation Channel

2) *Thermo-luminescent detectors*

For gamma dose measurement, in the range of few kGy, we used thermo-luminescent detectors of type TLD400 (CaF_2: Mn) obtained from Thermo-Fisher Scientific. The TLD400 post-irradiation reading protocol is performed with a Harshaw Model 3500 TLD reader (cf. Fig. 6), allowing the TLDs to be heated up to 400°C. The charge integrated in the TLD detector is read using the following sequence: preheating phase at 150 °C for 5 s, followed by a ramp-up to 350 °C at a rate of 10 °C.s^{-1} and maintaining this temperature for 30 s.

Prior to the irradiations, the TLD detectors were calibrated, at a dose range of several kGy, using a reference gamma field generated by the PAGURE and POSEIDON ^{60}Co sources at CEA Saclay. This calibration establishes the link between the integral charge Q (expressed in nC or counts) of the luminescent signal read post irradiation and the dose to which the detectors are exposed, which is represented by the reference quantity of Kerma air (in Gy). The obtained results were adjusted with rational model, defined as ratios of polynomials.

Fig. 6. Thermo-luminescent detectors acquisition bench.

As shown in Table II, two irradiations, 5 kW – 10 min (irradiation 1) and 5 kW – 5 min (irradiation 2), were performed in the CT and G25 irradiation channels. The TLD measurements were carried out in 3 phases: measurement of the background gamma (reactor shutdown), measurement during transients (divergence up to 5 kW then rod-drop) and finally a measurement during a constant power level of 5 kW. To determine the net dose integrated over constant power level, we subtract the dose integrated during the background and transient measurements.

TABLE II
TLD IRRADIATIONS IN BOTH CT AND G25 CHANNELS.

Date of irradiation	EXPERIMENT	Power level	Irradiation time	IC
24/06/2022	Background	0 W	1 h	5 axial positions in the CT and G25
27/06/2022	Divergence	5 kW	-	
24/06/2022	**1st irradiation**	5 kW	10 min	
27/06/2022	Background	0 W	2 h 49 min	
28/06/2022	**2nd irradiation**	5 kW	5 min	

Prior to the measurements, preliminary simulations, using the TRIPOLI-4® [16] computational model of the TRIGA reactor, were carried out to design the TLD measurements. Hence, the duration and power level were adjusted to obtain an integrated dose within the calibration and linear operating range of the TLD detectors (in the range of Gy to few kGy).

3) *Miniature ionization chamber*

To assess photon flux in the two-irradiation channels, we used a miniature ionization chamber (MIC) manufactured by PHOTONIS. It is a gas-filled (Argon at 5 bar) detector, with 3 mm diameter and 10 mm sensitive length, that is sealed to a mineral cable (cf. Fig. 7).

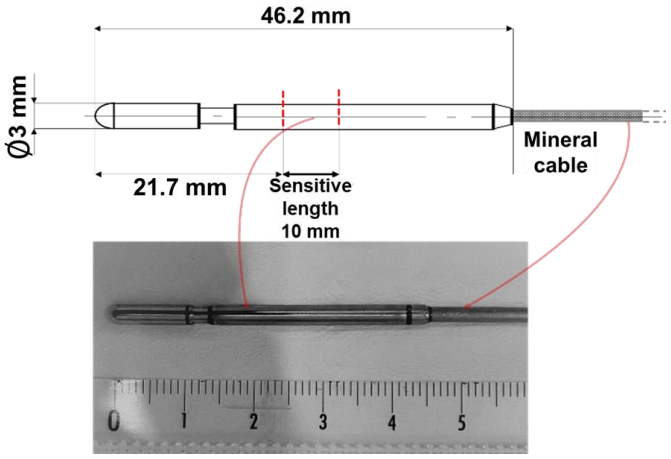

Fig. 7. Miniature ionization chamber used for measurements in TRIGA.

For current measurement and high voltage supply, a Keithley 6517B electrometer, controlled by a LabVIEW-based data acquisition application, was used. The bias voltage was set to 150 V (manufacturer's specified value) and the current was measured with a sampling rate of 1 Hz.

Different measurements with the MIC were carried out in the CT and G25 channels. At first, was positioned at the core center in order to verify the linearity of the measured current as a function of the reactor power. To do this, the power was gradually increased in steps ranging from 0 to 1800 kW, while allowing the power to stabilize at each step to verify any drifting in the measured signal. Then, the MIC was used to characterize the axial profile of the photon flux in the two-irradiation channels.

III. Results and discussions

The following sections are dedicated to the analysis of the experiments' results. Each type of measurements will be treated and analyzed and the associated uncertainties will be evaluated.

A. Activation measurements

At the end of the irradiation, the specific activity (in unit of Bq.mg^{-1}) of the radioisotopes formed during the irradiation process is evaluated using γ spectrometry measurements. By determining the number of counts under the total absorption peak, the activity A_j of a radioisotope is calculated by the following formula:

$$A_j = \frac{N(E_j)}{m I_\gamma(E_j)\varepsilon(E_j)T(E_j)t_a}\prod_i C_i \qquad (1)$$

where $N(E_j)$ is the number of counts in the absorption peak of energy E_j, m is the mass in g of the measured dosimeter, $I_\gamma(E_j)$ is the intensity of the photon emission, $\varepsilon(E_j)$ is the detector's efficiency for the photon with the energy E_j, $T(E_j)$ is the yield transfer factor for the photon with energy E_j, t_a the acquisition (counting) duration in s and $\prod_i C_i$ is the product of the correction coefficients of dead time, decay and coincidences. The activity profiles of the cobalt and nickel dosimeters irradiated in CT and G25 channels are presented in Fig. 8 and Fig. 9. The overall relative uncertainty associated to the activity at the end of irradiation is the quadratic combination of the relative uncertainties on each term of equation (1) assuming that the variables are independent of each other. A summary of these uncertainties (at 1σ) is presented in the following:

- The uncertainty in the determination of the net peak area combines both the uncertainties of counting rate and the background. This uncertainty is directly given by the acquisition software used and is of the order of 1% for all the dosimeters irradiated in the CT and G25.
- The uncertainty of the detector's efficiency is evaluated from the covariance data associated with the fourth-order polynomial fit of experimental data [15]. These uncertainties are around 1 to 2%.
- The uncertainties associated with the photon emission probabilities and decay uncertainties for cobalt and nickel dosimeters are generally very well-known and are around 0.04% for the radioactive constants and around 0.06% for the photon emission intensities [17].
- The coincidence correction was evaluated with the ETNA software developed by Laboratoire National Henri Becquerel (LNHB). The uncertainty on the coincidence correction is estimated at 10% of the corrective term (LNHB recommendation) which corresponds to a relative uncertainty of 0.1%.
- The yield transfer factor, which corrects the difference between the dosimeter measurement geometry and the calibration geometry, was estimated by TRIPOLI-4 calculations. The associated uncertainty is around 0.5% for different calibration configuration.

Finally, the relative uncertainty on the activity at the end of irradiation varies from 1% to 3%.

The axial profiles of the cobalt and nickel dosimeters present a maximum around the reactor core mid-plane and decrease symmetrically as moving away from the core center toward the graphite reflectors at the top and bottom of the FE.

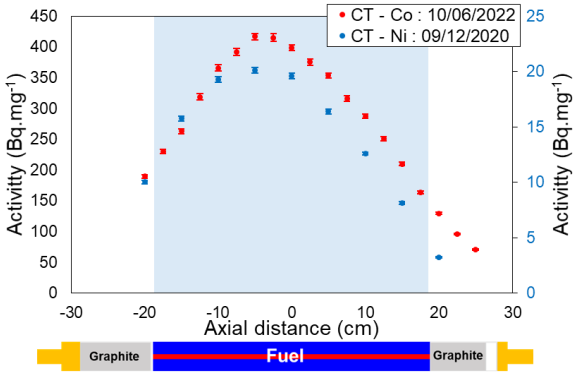

Fig. 8. Cobalt and nickel activities measured in the CT irradiation channel. The area marked in blue corresponds to the active fuel region of the standard FE.

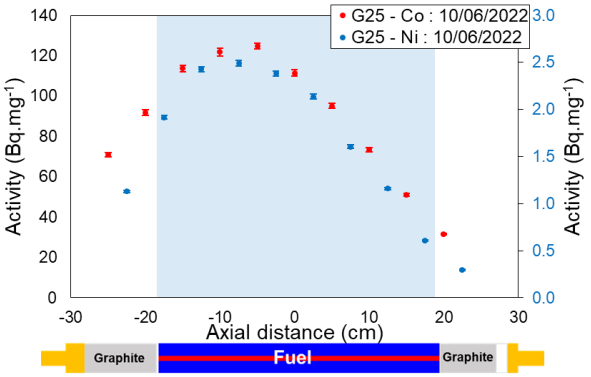

Fig. 9. Cobalt and nickel activities measured in the G25 irradiation channel.

B. TLD measurements

The net integrated dose, by the TLDs, over a constant power level and corrected for background and transient is obtained by the following formula:

$$D_{net} = D_{irr} - D_{div} - D_{Bd}\left(\frac{t_{irr} - t_{div}}{t_{Bd}}\right) \qquad (2)$$

where D_{net} is the net dose integrated during the constant power level (kGy), D_{irr} is the integrated dose over the entire irradiation duration, D_{div} is the dose integrated during the transient phase, D_{Bd} is the dose integrated during the background measurement, t_{irr}, t_{div} and t_{Bd} are respectively the irradiation, the transient and the background durations (see Table II).

In order to be qualitatively compared, the net doses are normalized to the average energy (in W.s^{-1}) released during the irradiation process. This normalization is calculated as follows:

$$D_{i,norm} = \frac{D_{i,net}}{\overline{P_{irr}} \times t_{irr}} \qquad (3)$$

where $D_{i,net}$ is the net dose at the position "i" in kGy, $\overline{P_{irr}}$ and t_{irr} are respectively the power level and the irradiation duration.

Fig. 10 and Fig. 11 summarize the results of the net dose rates normalized to the irradiation power. From these results, one can conclude that:

- The maximum dose rate in the CT is around (6.44 ± 0.75) $\times 10^{-7}$ kGy.W^{-1}.s^{-1} for 10 min irradiation at 5 kW.
- For the G25, the maximum dose rate is around (1.40 ± 0.14) $\times 10^{-7}$ kGy.W^{-1}.s^{-1}.
- The uncertainties associated with the dose measurement vary from 7 to 15% (1σ) and are primarily due to the uncertainties associated with the calibration of the TLDs.

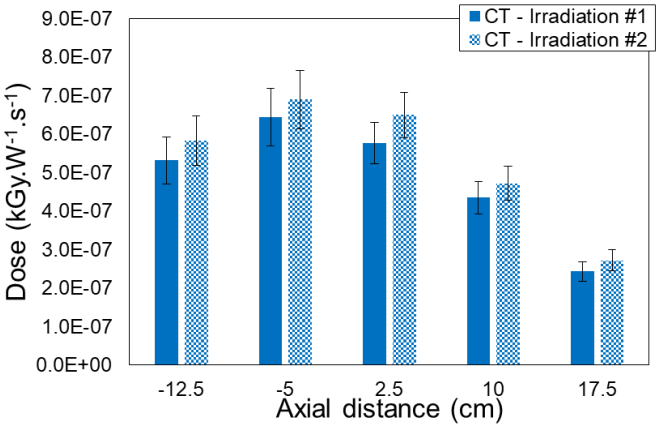

Fig. 10. Results of doses measurements in the CT channel, the solid and dotted lined bars stand for each irradiation.

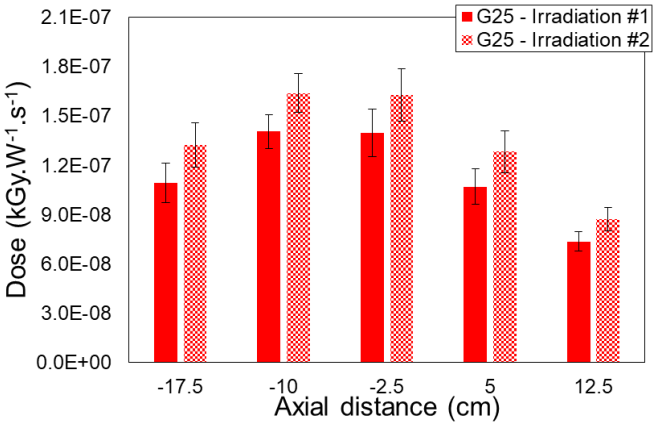

Fig. 11. Results of doses measurements in the G25 channel, the solid and dotted lined bars stand for each irradiation.

C. *MIC measurements*

The axial current profiles measured by the MIC are presented in Fig. 12 and Fig. 13. For each channel, two irradiations at the same power level were performed in order to evaluate the reproducibility of the measurement. The uncertainties associated with these measurements are directly estimated from the variation of the measured current and are around 1% (k=1). Comparing these profiles, one can observe that:

- The profiles in the CT and G25 have maxima at -6 cm below the mid-plane of the reactor core and decrease away from this maximum.
- The measurements are reproducible and consistent given the associated uncertainties.

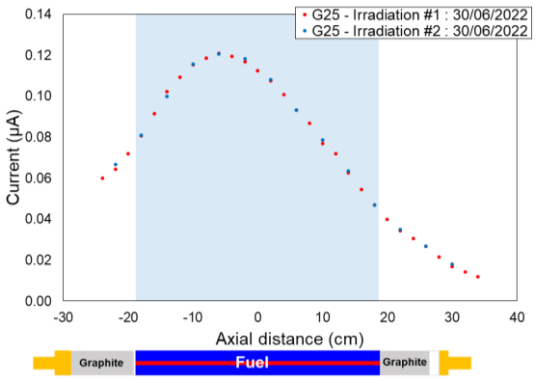

Fig. 12. Results of MIC current measurements in the CT channel.

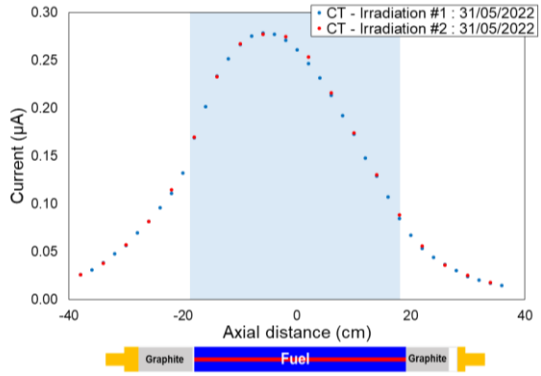

Fig. 13. Results of MIC current measurements in the G25 channel.

D. *Inter-comparison of measurements*

To compare the neutron and photon measurements with each other, the axial profiles were normalized to the maximum value in each channel. Fig. 14 and Fig. 15 illustrate the normalized neutron and photon profiles. The results show that:

- For the CT, the neutron and photon profiles show a maximum between -6 cm and 2.5 cm below the core mid-plane.
- For the G25, the maximum is between -10 cm and -2.5 cm below the core mid-plane.
- The different profiles, around the core mid-plane, are consistent with each other.

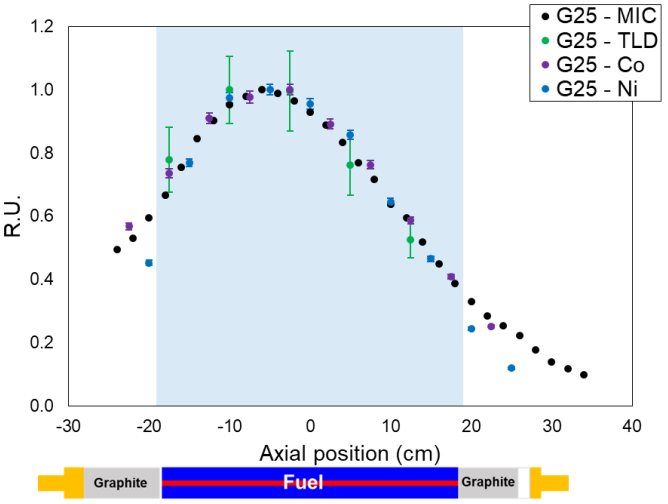

Fig. 14. Inter-comparison of measurements in the CT channel.

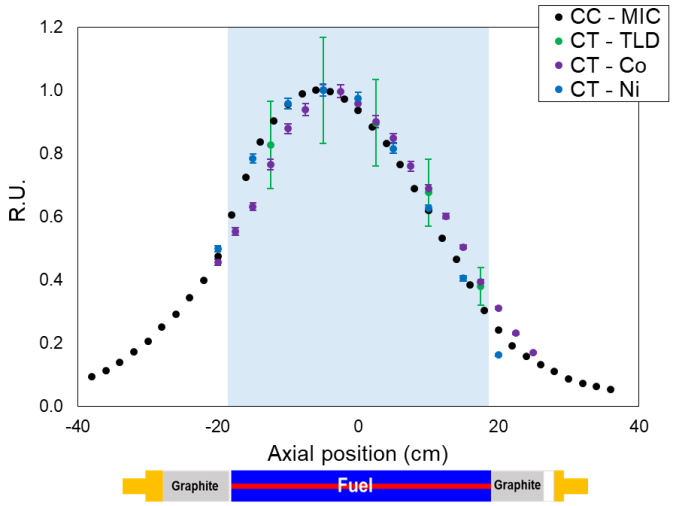

Fig. 15. Inter-comparison of measurements in the G25 channel.

IV. Conclusion and perspectives

In this paper, the experimental characterization of two in-core irradiation channels of the CNESTEN's TRIGA Mark II reactor is presented. Three different types of detectors (activation detectors, TLD and MIC) were used to assess neutron and photon flux measurements. For each type of measurement, the results are analyzed and the associated uncertainties are evaluated and quantified. Indeed, the inter-comparison of measurements show a qualitatively good consistency within the associated uncertainties at 1 or 2σ.

This work should be continued by a thorough interpretation of these measurements using Monte-Carlo calculations. The comparison between the calculated and measured values will allow the evaluation of discrepancies and biases and will extend the experimental validation basis of the TRIGA computational models (developed with TRIPOLI-4® and MCNP codes).

References

[1] B. El Bakkari, B. Nacir, T. El Bardouni, C. El Younoussi, Y. Boulaich, et H. Boukhal, « Feasibility analysis of I-131 production in the Moroccan TRIGA research reactor », *Annals of Nuclear Energy*, vol. 78, p. 140-145, avr. 2015, doi: 10.1016/j.anucene.2014.11.044.

[2] A. Fllaoui *et al.*, « Validation of a New Design of Tellurium Dioxide-Irradiated Target », *Nuclear Engineering and Technology*, vol. 48, nº 5, p. 1273-1279, oct. 2016, doi: 10.1016/j.net.2016.05.004.

[3] T. Žagar, M. Božič, et M. Ravnik, « Long-lived activation products in TRIGA Mark II research reactor concrete shield: calculation and experiment », *Journal of Nuclear Materials*, vol. 335, nº 3, p. 379-386, déc. 2004, doi: 10.1016/j.jnucmat.2004.07.047.

[4] A. Räty *et al.*, « Characterization measurements of fluental and graphite in FiR1 TRIGA research reactor decommissioning waste », *Nuclear Engineering and Design*, vol. 353, p. 110198, nov. 2019, doi: 10.1016/j.nucengdes.2019.110198.

[5] M. Ferrari, A. Zenoni, Y. Lee, et Y. Hayashi, « Characterization of a polyphenyl ether oil irradiated at high doses in a TRIGA Mark II nuclear reactor », *Nuclear Instruments and Methods in Physics Research Section B: Beam Interactions with Materials and Atoms*, vol. 497, p. 1-9, juin 2021, doi: 10.1016/j.nimb.2021.03.021.

[6] M. Cagnazzo, A. Borio di Tigliole, H. Böck, et M. Villa, « Fission products detection in irradiated TRIGA fuel by means of gamma spectroscopy and MCNP calculation », *Applied Radiation and Isotopes*, vol. 135, p. 123-130, mai 2018, doi: 10.1016/j.apradiso.2018.01.027.

[7] M. A. Allaf, S. Ş. Lüle, et Ü. Çolak, « The development of TM2-RIA code for TRIGA type research reactors », *Annals of Nuclear Energy*, vol. 145, p. 107545, sept. 2020, doi: 10.1016/j.anucene.2020.107545.

[8] M. R. Omar, J. A. Karim, et T. L. Yoon, « The development of a multigroup Monte Carlo code for TRIGA reactors », *Nuclear Engineering and Design*, vol. 342, p. 99-114, févr. 2019, doi: 10.1016/j.nucengdes.2018.11.039.

[9] K. Ambrožič et L. Snoj, « JSIR2S code for delayed radiation simulations: Validation against measurements at the JSI TRIGA reactor », *Progress in Nuclear Energy*, vol. 129, p. 103498, nov. 2020, doi: 10.1016/j.pnucene.2020.103498.

[10] E. Chham *et al.*, « Fuel reloads optimization for TRIGA research reactor using Genetic Algorithm coupled with neutronic and thermal-hydraulic codes », *Progress in Nuclear Energy*, vol. 133, p. 103637, mars 2021, doi: 10.1016/j.pnucene.2021.103637.

[11] V. Radulović, R. Jaćimović, A. Pungerčič, I. Vavtar, L. Snoj, et A. Trkov, « Characterization of the neutron spectra in three irradiation channels of the JSI TRIGA reactor using the GRUPINT spectrum adjustment code », *Nuclear Data Sheets*, vol. 167, p. 61-75, juill. 2020, doi: 10.1016/j.nds.2020.07.003.

[12] B. El Bakkari, T. El Bardouni, O. Merroun, Ch. El Younoussi, Y. Boulaich, et E. Chakir, « Development of an MCNP-tally based burnup code and validation through PWR benchmark exercises », *Annals of Nuclear Energy*, vol. 36, nº 5, p. 626-633, mai 2009, doi: 10.1016/j.anucene.2008.12.025.

[13] X-5 Monte Carlo Team, « MCNP – A general Monte Carlo N-Particle Transport Code, Version 5, LA-UR-03-1987. », 2004.

[14] B. El Bakkari *et al.*, « Monte Carlo modelling of TRIGA research reactor », *Radiation Physics and Chemistry*, vol. 79, nº 10, p. 1022-1030, oct. 2010, doi: 10.1016/j.radphyschem.2010.04.016.

[15] H. Ghninou *et al.*, « Characterization of Neutron Reaction Rates in Different Irradiation Channels of the CNESTEN's TRIGA Mark II Research Reactor », *IEEE Transactions on Nuclear Science*, vol. 69, nº 7, p. 1806-1814, juill. 2022, doi: 10.1109/TNS.2022.3174673.

[16] E. Brun *et al.*, « TRIPOLI-4®, CEA, EDF and AREVA reference Monte Carlo code », *Annals of Nuclear Energy*, vol. 82, p. 151-160, août 2015, doi: 10.1016/j.anucene.2014.07.053.

[17] « NUCLÉIDE-LARA on the web (2022) ». http://www.nucleide.org/Laraweb/index.php (consulté le 25 août 2022).